

Relative importance of convection and diffusion in binary liquid systems subject to small horizontal temperature gradients

Thomas C. Van Vechten and Carl Franck

Laboratory of Atomic and Solid State Physics and the Materials Science Center, Cornell University, Ithaca, New York 14853-2501

(Received 24 February 1992; revised manuscript received 16 June 1993)

By comparing the convection and diffusion transport times of a binary liquid mixture contained in a rectangular box subjected to a small horizontal temperature gradient we roughly estimate the size of an accidental temperature gradient that can be allowed without keeping an experiment away from effective equilibrium. This approximate criterion is then tested against an experiment that is independently known to have equilibrated [G. Maisano, P. Migliardo, and F. Wanderligh, *J. Phys. A* **9**, 2149 (1976)], and we find that the experiment was close to our predicted borderline.

PACS number(s): 47.27.Te, 05.70.Ln, 05.70.Jk

I. INTRODUCTION

The observation of thermal equilibrium phenomena in binary liquid mixtures continues to hold great interest. Some investigations, such as the measurement of the bulk coexistence curve (see the review article of Kumar, Krishnamurthy, and Gopal [1]), can tolerate qualitatively significant departures from thermal equilibrium. In particular, one does not require formation of gravity-induced gradients in the species concentration. Other work may require a much closer approach to true thermodynamic equilibrium. For example, in the case of gravity-thinned wetting for a liquid at bulk coexistence, these concentration gradients must equilibrate [2]. Thus studies of binary liquid systems are often complicated by the difficulty in establishing that a sufficient degree of equilibrium has been achieved. Here we discuss the effect of convection due to the small horizontal temperature gradients that will inevitably occur in the environment of a real sample cell, and the possibility that this will drive the system out of effective equilibrium. Although such convection effects are lurking in many experiments, an estimate of their importance has been lacking. We will suggest a criterion based on a solution of the Navier-Stokes equations for the acceptable size of horizontal temperature gradients. This test will then be examined by applying it to experiments that we know came to equilibrium.

If the liquid did not convect the distribution of species would be governed by diffusion. This is described by the diffusion flux density vector for a particular component of the mixture [3]:

$$\mathbf{j} = \rho D [\nabla C + (k_T/T)\nabla T + (k_p/p)\nabla p]. \quad (1)$$

Here ρ is the density, D is the mutual diffusion constant, k_T is the thermal diffusion ratio, T is the temperature, k_p is the barodiffusion ratio, p is the pressure, and C is the concentration by mass fraction of one species (in this paper the denser one). When a steady state is attained in a closed system, the flux will be zero and temperature or

pressure gradients will produce a concentration gradient. For temperature gradients this is called the Soret effect. For binary liquids in the vicinity of their phase separation critical point k_T and k_p both diverge [4,5], which means that these effects can be important. Barodiffusion is an integral part of the equilibration of a binary liquid system, forming the vertical density gradients mentioned in the first paragraph. Since it takes place by diffusion over macroscopic distances, the time scale for equilibration can be long (weeks or months) [6]. Thus a convective flow that can overturn the liquid in times short compared to this is important, even though the flow speed may be only tens of nanometers per second.

The real flow will be determined by the density variations produced by thermal expansion, mechanical compression, and the concentration gradients due to barodiffusion and the Soret effect. If the liquid in question has a free interface, then temperature-induced gradients in the surface tension can also produce convection; this effect is called Marangoni convection. Because we are interested in a case where the liquid has no free surface, we do not need to include Marangoni convection. In the samples that we are considering here, the Soret effect will segregate the denser species into the warmer regions of the fluid, and sufficiently near the critical phase transition, the equilibrium value of this concentration gradient would produce a horizontal density gradient larger than (and with the opposite sign to) the horizontal density gradient due to thermal expansion. This would be expected to have a very considerable influence on the flow. However, because the cells we are interested in here are wider than they are tall, the time needed for the barodiffusion to equilibrate will be much shorter than the time for the Soret gradient, so that the experiment will be ended before this becomes significant and we neglect it here. In a more general work these effects would both be considered.

In order to obtain a convenient analytic result we further simplify the problem by considering the concentration gradient to be determined by barodiffusion and any intended external mixing done by the experimenter alone.

We will neglect the effect of the convective flow on the species distribution. This means that our results are not self-consistent. We feel that this is a justifiable approximation for extremely slow flows, but it would not hold for flows that are significant compared to diffusion. We will also make the Boussinesq approximation, that is, we will assume that temperature changes are small enough that, except for density, we can regard fluid properties as temperature independent, as discussed in Ref. [7].

The temperature gradient of interest will presumably vary with time. If we consider the Fourier transform of this signal giving the amplitude of the temperature gradient as a function of frequency, we can separate it into three frequency regimes: The low-frequency limit has periods that are long compared to the time of the experiment; these will be labeled dc temperature gradients. The high-frequency limit has periods that are short compared to the time needed for heat to pass through the sample by conduction and advection. The temperature fluctuations that are long enough lived to establish themselves throughout the cell but those that do not last as long as the experiment will be placed in the intermediate-frequency regime.

We expect that the high-frequency temperature fluctuations will have little effect on the distribution of mass in the sample. Since heat can conduct through a typical sample on a time scale of minutes, we can neglect fluctuations with frequencies higher than 10 mHz or so, even if the amplitude at these frequencies is larger than that of the low-frequency fluctuations. For simplicity we will at first consider only the very-low-frequency fluctuations which can be treated as constant over the period of the experiment. Intermediate-frequency fluctuations, such as those that might have periods of a day, will be neglected. Because, even though they last long enough to pervade the fluid and establish a flow, they would not transport material as far or as consistently as a constant flow. Nevertheless, this regime might still be interesting and significant.

Small horizontal temperature gradients are more interesting or troublesome than the more heavily studied vertical temperature gradients. A vertical temperature gradient must exceed a certain magnitude in order to drive convective flow, although in a two-component liquid this threshold can be much smaller than it is in the more familiar one-component case, if the Soret effect or the initial conditions put the denser species at the top [8,9]. This means that a good experiment can be conducted in which no convection due to vertical temperature gradients takes place. However, a horizontal temperature gradient will always produce convection (in an incompressible liquid) regardless of the size or the sign of the gradient [10]. Thus a clever experimentalist will still have to contend with this flow.

Since convection will be taking place inside the sample, it is important to determine if the system has approached equilibrium in spite of convection or has merely reached a steady state. To make this determination one must have both a knowledge of the velocity field inside the fluid and an appreciation of the significance of that velocity for the particular system of interest.

II. THE EXISTENCE OF WELL ENOUGH EQUILIBRATED EXPERIMENTS

In the presence of horizontal temperature gradients the system will be out of thermal equilibrium on both the microscopic scale of heat flow and entropy generation by molecular collisions and on the macroscopic scale of coherent flow throughout the system. For small temperature gradients it is only the macroscopic departure from equilibrium that concerns us here. However, this departure will not be qualitatively significant in a particular experiment if the temperature gradient has been brought to such a low value that further reducing the gradient would not noticeably change the results.

One example is the observation of gravitational concentration gradients due to barodiffusion in aniline plus cyclohexane by Maisano, Migliardo, and Wanderligh [6]. They observed gradients similar to the expected equilibrium gradients in an environment where the temperature gradients were less than 0.5 mK/cm. These temperature gradients could not have produced vigorous convection because if they had, the vertical concentration gradient would not have formed. A small fluid element that at the beginning of the experiment was near the bottom of the sample and thus grew to be poor in cyclohexane, would instead have traveled repeatedly from bottom to top and back, and thus would have spent as much time enriching itself in cyclohexane as it did losing it. We will use this successful experiment to evaluate our standards for convective disruption of thermal equilibrium.

III. FLUID DYNAMICS AND TIME SCALES

The velocity field can be directly measured in principle, but this is impractical with conventional techniques such as seeding the flow with neutrally buoyant particles for the small velocities under consideration. If the temperature gradient and density profile of the fluid are known, then a calculation by Hart [11] or Thangam, Zebib, and Chen [12] enables us to predict the velocity field, for the simple geometry of a rectangular slot of finite horizontal width in one direction but infinite height. It is assumed that the vertical concentration gradient has some constant known value, which represents the gradient due to barodiffusion, and it is assumed that the sample is broad enough in the horizontal direction perpendicular to the temperature gradient to be considered infinite. Under these assumptions Hart and Thangam, Zebib, and Chen solved the linearized Navier-Stokes equations.

We have extended Hart's work [13] by introducing a finite vertical distance scale to the flow. The vertical concentration gradient is still assumed to be constant in space and time. For a more detailed discussion of the fluid dynamics see the Appendix. For our purposes a crucial result from both Hart's and our treatments is that vertical density gradients can greatly reduce the convective velocity. The vertical velocities calculated for different density gradients in a particular system as a function of horizontal position demonstrate this in Fig. 1.

In our calculations of the velocity we assumed that it could be described by a stream function written as a

product of a function of the horizontal position times a cosine of the vertical position. There are a number of studies of numerical solutions of the case of two component fluids heated from the side contained in rectangular slots of finite height [14,15] but the reports do not give the complete velocity field for the low-temperature gradient, almost stagnant fluids that are needed for our calculations. These studies do suggest that there would be convection cells confined to the top and bottom of the

container, and that the magnitude of the velocity would be small in the middle of the container. Since we are primarily concerned with the vertical distribution of concentration within the container, we focus our attention on the large central region of the flow. Here we present an analytic result which can be easily calculated for any small temperature or density gradient one might need to consider.

Once the velocity has been established, its significance can be found by comparing the magnitude of fluid flow to diffusion. The criterion that we would suggest to discriminate between diffusion-dominated systems and convection-dominated systems is to compare the time for a molecule to diffuse the vertical height of the sample with the time needed for convection to carry a molecule the same distance (following Ref. [2]). One would then expect that if the convection time were shorter than the diffusion time, the system would evolve into a flowing steady state that would be far from equilibrium, while if the temperature gradient were small and the convection time long, diffusion would dominate, until thermal equilibrium is effectively attained.

IV. CONSTRUCTION OF THE GENERAL TRANSPORT MECHANISM REGIME DIAGRAM

Thus we will produce a regime diagram showing the space of initial conditions for an experiment and indicating the relative time for convection and diffusion for each point. An experiment that begins well in the diffusion regime should equilibrate while both diffusion and convection will need to be considered for experiments near the boundary. Experiments far in the convection regime would be dominated by flow effects. In order to apply our criterion it is a straightforward matter to substitute into Eq. (3) and its supporting Eqs. (4)–(13). It is unfortunate that the resultant diagram is particular to any given experiment. Then measurements need to be made on the temperature bath and the mechanical compressibility of the liquid found in order to determine the initial conditions of interest for each experiment.

The time for convection to carry a molecule across the sample is the height of the sample divided by the flow velocity. Since the flow velocity varies with position within the cell, this does not give a single time. Consequently we will either integrate over space to obtain a velocity representative of the entire flow or we will consider the sample to be divided into smaller regions throughout which we can treat the velocity as constant. We would then determine the behavior of representative regions of the flow. We will call either of these velocities V_M , the measure of the velocity. Since we are primarily concerned that each small fluid element have a constant height so that it can come to the equilibrium concentration in response to barodiffusion, we want a measure of the flow that gives the total circulation. We integrate over the horizontal direction the absolute value of the velocity at the midplane, where the flow is vertical, to get a simple measure of this.

The time τ for a molecule to diffuse a distance L is taken to be given by

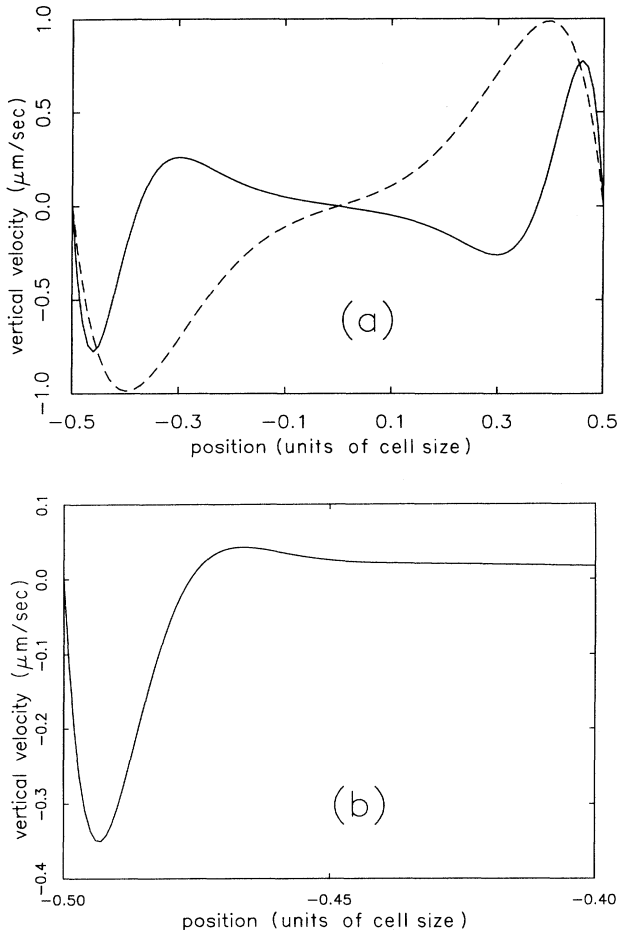


FIG. 1. The vertical velocity as a function of horizontal position for a box with width twice its height filled with aniline plus cyclohexane heated from the side. The average temperature of the cell is 0.54 K above the critical phase transition temperature. The sample was prepared at the critical concentration. The hot wall is at $x = -0.5$, the cold wall is at $x = +0.5$. The velocity was calculated at the horizontal midplane ($z = 0$) of the container. The dashed curve in (a) is the velocity of a liquid with a vertical density gradient equal to 1×10^{-14} g/cm⁴; this gradient can be considered to represent the small limit. The solid curve in (a) is ten times the velocity of a fluid with $\nabla\rho = 4.9 \times 10^{-8}$. This gradient is the mechanical settling, as described in the text. The solid curve in (b) is the velocity of a fluid with $\nabla\rho = 1.3 \times 10^{-4}$; this represents the barodiffusion gradient. Note that in case (b) the velocity is only significantly near the walls and the axes have been truncated and magnified accordingly.

$$\tau = \frac{L^2}{\pi^2 D}, \quad (2)$$

where D is the mutual diffusion constant which goes to zero near the critical phase transition point [16]. The π^2 comes from the solution of the diffusion equation under the assumption that the species concentration varies only in the vertical direction.

Using our extension of the theory of Hart for the velocity as a function of temperature gradient and vertical density gradient, we took the convection time to be the vertical height of the sample cell divided by either the horizontal integral of the absolute value of the velocity at the midplane of the container or the velocity of the fluid at a particular point x_0, z_0 . Setting this equal to the diffusion time above and then solving for the corresponding temperature gradient we find

$$\nabla T = \frac{\pi^2 \nu(\epsilon) D(\epsilon)}{g \alpha(\epsilon) L X^3 V_M}, \quad (3)$$

where

$$V_M = \int_{-1/2}^{1/2} |w(x, 0)| dx \quad (4)$$

or

$$V_M = w(x_0, z_0) \quad (5)$$

and from the Appendix we have

$$w(x, z) \equiv [E_p \gamma \sinh(\gamma x) + E_1 \cosh(\mu x) \sin(\lambda x) + E_2 \sinh(\mu x) \cos(\lambda x)] \cos(\gamma z) \quad (6)$$

with

$$E_1 \equiv \frac{2E_p}{\mu \sin(\lambda) + \lambda \sinh(\mu)} \times [(\mu^2 + \lambda^2) \cosh(\gamma/2) \sinh(\mu/2) \cos(\lambda/2) - \mu \gamma \sinh(\gamma/2) \cosh(\mu/2) \cos(\lambda/2) - \lambda \gamma \sinh(\gamma/2) \sinh(\mu/2) \sin(\lambda/2)], \quad (7)$$

$$E_2 \equiv \frac{2E_p}{\mu \sin(\lambda) + \lambda \sinh(\mu)} \times [-(\mu^2 + \lambda^2) \cosh(\gamma/2) \cosh(\mu/2) \sin(\lambda/2) + \mu \gamma \sinh(\gamma/2) \sinh(\mu/2) \sin(\lambda/2) - \lambda \gamma \sinh(\gamma/2) \cosh(\mu/2) \cos(\lambda/2)], \quad (8)$$

where

$$\mu \equiv \frac{1}{\sqrt{2}} (\sqrt{\gamma^4 - R_s} + \gamma^2)^{1/2}, \quad (9)$$

$$\lambda \equiv \frac{1}{\sqrt{2}} (\sqrt{\gamma^4 - R_s} - \gamma^2)^{1/2}, \quad (10)$$

$$E_p \equiv \frac{2\gamma}{\pi R_s \sinh(\gamma/2)}, \quad (11)$$

$$\gamma \equiv \frac{\pi}{L/x}, \quad (12)$$

$$R_s \equiv \frac{g \beta (\partial C / \partial z) L^4}{D(\epsilon) \nu(\epsilon)}. \quad (13)$$

Here X is the horizontal size of the sample cell, x is the horizontal coordinate expressed in units of X , the cell walls have $x = \pm \frac{1}{2}$, \hat{z} is the vertical direction, L is the vertical height of the sample in units of X , with $z = 0$ at the middle, V_M is a measure of the velocity, $w(x, z)$ is the scaled vertical component of the velocity (to get the actual velocity multiply this by $g \alpha X^2 \Delta T / \nu$), ν is the kinematic viscosity, α is the thermal expansivity, D is the mutual diffusion constant, T_c is the critical phase transition temperature, ϵ is the reduced temperature identically equal to $|T - T_c| / T_c$, g is the gravitational acceleration, C is the mass concentration of the denser species (aniline, in this paper), $\beta = (1/\rho)(\partial \rho / \partial C)$ is the coefficient of volumetric expansion, and ΔT is the horizontal temperature difference across the cell. We can convert the concentration gradient to a mass density gradient as follows: $\nabla \rho = \Delta \rho \nabla C$, where we assert that $\partial \rho / \partial C = \Delta \rho$, the mass density difference between the two pure liquids, i.e., there is no significant volume change upon mixing.

V. DRAWING THE PARTICULAR TRANSPORT MECHANISM REGIME DIAGRAM

Evaluating Eq. (3) for the aniline-plus-cyclohexane system gives the horizontal temperature gradient for which the diffusion time would equal the convection time as a function of the vertical mass density gradient present in the sample. This is shown in Fig. 2. All curves were calculated with $z = 0$ where the velocity is the strongest. Note that the smooth curves represented with solid or dashed lines are based on the convection time calculated from the horizontal spatial integral of the absolute value of the velocity [V_M is given by Eq. (4)]. The dash-dotted curves are calculated using the velocity at the horizontal position indicated for each curve. For these curves V_M is given by Eq. (5). Recall that $x = 0.5$ is the position of a wall and $x = 0$ is the center of the cell. The spikes on these curves reflect the existence of zeros in the velocity function. The position of the zeros in space varies with the vertical density gradient.

The calculation was done for a system with an average temperature 0.54 K above the critical phase-transition temperature, but other temperatures also used by Maisano, Migliardo, and Wanderligh (0.19 and 0.07 K above T_c) give curves with very similar behavior in the regime where ∇T increases with $\nabla \rho$, which is the most relevant one here.

We used data on the kinematic viscosity of aniline plus cyclohexane taken by Arcovito *et al.* [17]. Data giving the thermal expansivity at temperatures near the critical point could not be found, so that we estimated the possible range of singular behaviors of the thermal expansivity of the mixture by investigating literature descriptions of the thermal expansivity for a few binary liquids [18–20] and then scaled them so that the nonsingular part was the same magnitude as the nonsingular expansivity of aniline plus cyclohexane, which we took to be the average of the thermal expansivities of pure aniline and cyclohexane weighted by the mole fractions at the critical composition [21].

As indicated before, these curves are particular to the

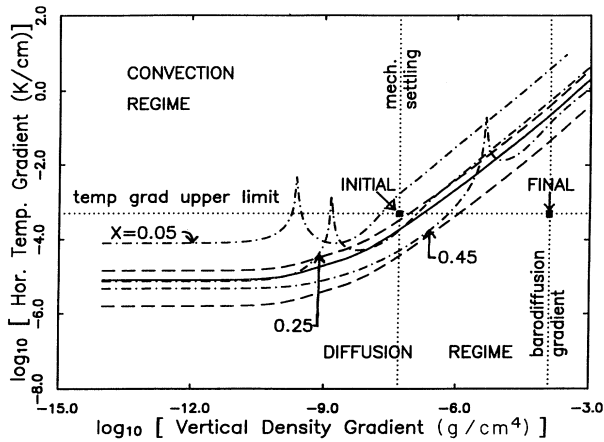


FIG. 2. Predicted transport mechanism regime diagram for a binary liquid mixture of aniline plus cyclohexane heated from the side. The sample cell is 1 cm tall and 2 cm wide. The temperature is 0.54 K above the critical mixing temperature and the concentration is critical [6]. The solid curve is the predicted regime boundary based on the horizontal spatial integral of the absolute value of the velocity; the dashed curves on either side represent the uncertainty. Equal fractional uncertainties also apply to the dash-dotted curves. These dash-dotted curves are the regime boundary for fluid at the horizontal positions indicated. Here $x=0$ is the center of the cell and $x=0.5$ is a wall. The vertical lines show the significant vertical density gradients that might be present in the cell: the left one mechanical settling of a fluid with homogeneous species distribution and the right one equilibrium barodiffusion. The horizontal line is the upper bound on the temperature gradient provided by the temperature bath used by Maisano, Migliardo, and Wanderligh [6].

cell geometry and fluid properties used by Maisano, Migliardo, and Wanderligh, and different systems would be expected to have different curves. To examine a different experiment one would need to evaluate the set of Eqs. (3)–(13) using the parameters of that system.

The uncertainty of our result has several sources: the non-self-consistency of the fluid dynamics due to the neglect of the precise effect of the flow on the concentration gradient, our ignorance of the behavior of the thermal expansion coefficient of the aniline-plus-cyclohexane mixture near the critical transition point, the errors introduced in our fluid dynamics when we consider only the first term of the Fourier expansion of the temperature and when we place a free-slip boundary at the top and bottom of the fluid, and the error introduced by our choice of technique to spatially average the flow. The magnitude of the thermal expansivity error can be roughly determined by examining the range of critical behaviors exhibited by other binary liquid systems. The magnitude of the other errors is more difficult to establish without better treatments of the fluid dynamics. Since we do not know how large these errors should be, we will not attempt to include them in Fig. 2. Thus the errors indicated by the dashed curves about the spatial average (solid) curve includes only the error in thermal expansion, even though other errors may be more important. To further simplify the figure, the thermal expansion errors

are not shown for the curves calculated for particular positions.

VI. FINDING THE INITIAL CONDITIONS

Once the transport mechanism regime diagram has been found we need to establish the starting position of the experiment in question on that plane. To do this we need the horizontal temperature gradient produced by the imperfections in the temperature-regulating system and the vertical density gradient present at the beginning of the experiment.

These will depend on both the history and environment of the cell. Maisano, Migliardo, and Wanderligh placed a rectangular sample 4 cm wide \times 2 cm deep \times 1 cm tall in a temperature bath with temperature gradients less than 0.5 mK/cm and stirred the sample. After the stirring was stopped, a vertical density gradient was observed to form slowly. Thus we take the initial conditions for the experiment to be $\nabla T \approx 5 \times 10^{-4}$ K/cm and $\nabla C = 0$. Finally, $\nabla \rho$ needs to be established.

Placing the initial position on the temperature axis is relatively straight forward. The horizontal line on Fig. 2 gives the upper bound cited by Maisano, Migliardo, and Wanderligh of the temperature gradient present in the cell. The intersection of this line with any curve locates the boundary between the diffusion dominated regime (to the right) and the convection regime (to the left) for the fluid described by that curve.

Now we wish to consider the initial conditions regarding vertical density gradients. Even though the initial ∇C is zero we do not expect that $\nabla \rho$ would be exactly zero. This is because the extra pressure on the lower regions of the liquid due to the weight of overlying liquid will (slightly) compress the lower liquid. This gradient is given by

$$\left(\frac{\partial \rho}{\partial z} \right)_0 = \frac{\rho^2 g}{B} \quad (14)$$

Here B is the bulk modulus $= \rho(\partial p / \partial \rho)$. To derive Eq. (14), we replace $\partial p / \partial \rho$ by $\nabla p / (\partial \rho / \partial z)$ where ∇p is the gravitational pressure gradient. Using the adiabatic compressibility in place of the isothermal compressibility, we extract a value for B from the measured speed of sound in aniline plus cyclohexane [22].

Because we have been treating the liquid as incompressible, we have been able to take the density to depend on the concentration and temperature alone. To account for the density variation due to mechanical settling we will insert the small but nonzero compressibility of the real liquid into our treatment of an incompressible liquid by the *ad hoc* assumption that we can replace the actual concentration as a function of position $C(r)$ with an effective concentration $\tilde{C}(r)$, which would give the model liquid, at a minimum, the same vertical density gradient $[(\partial \rho / \partial z)_0]$ that the real, well-mixed compressible liquid would have, as follows:

$$\nabla \tilde{C} = \nabla C + \frac{\left(\frac{\partial \rho}{\partial z} \right)_0}{\Delta \rho} \quad (15)$$

We do this because the mechanical compression of the liquid would produce a density gradient that would be important in stabilizing the system against convection, but since the flow velocities considered here are much less than the speed of sound in the media the compressibility will not be important to the rest of the fluid dynamics. Note that except at the beginning of the experiment when the liquid has just been well mixed the concentration contribution to the density gradient will be much larger than the mechanical gradient so that $\bar{C} \cong C$.

Then the vertical line on the left-hand side of Fig. 2 is the density gradient due to mechanical settling of the slightly compressible liquid if the species concentration were uniform. The initial position of Maisano, Migliardo, and Wanderligh's experiment in this space is thus the intersection of the horizontal and leftmost vertical lines. This appears to be in the boundary between the diffusion and convection dominated regimes; however, we know from the final result of the experiment that diffusion established the expected equilibrium barodiffusion gradient in the system.

The rightmost vertical line locates the calculated vertical density gradient due to equilibrium species barodiffusion (it is actually the sum of the mechanical settling and barodiffusion terms, but since barodiffusion is so significant in this system, the mechanical settling can be neglected; this might not be true for other samples). This value is found by setting the Eq. (1) [3] equal to zero (since this is an equilibrium calculation). Doing so for the vertical direction, in which we will take the temperature gradient to be zero, we find

$$\nabla C = -(k_p/p)\nabla p \quad (16)$$

The pressure gradient is ρg because the sample is in the Earth's gravitational field. Thus we find that $\nabla \rho = \Delta \rho \nabla C$ should be $1.3 \times 10^{-4} \text{ g/cm}^4$, in agreement with Maisano, Migliardo, and Wanderligh's interferometrically measured value of $1.2 \times 10^{-4} \text{ g/cm}^4$. This agreement is a strong indication of thermal equilibrium.

VII. INTERPRETATION

In summary, we expect that immediately after stirring Maisano, Migliardo, and Wanderligh's experiment would reach a regime where both convection and diffusion are important. We experimentally know, but our criterion does not predict or counterindicate, that diffusion dominates the system, at least at long times.

We regard this analysis of the Maisano-Migliardo-Wanderligh experiment as weak confirmation of the diffusion-time-convection-time comparison as a test of the importance of the perturbation caused by dc horizontal temperature gradients. If a substantial majority of the fluid had clearly been in the diffusion regime, we would have stronger support. We take comfort from the fact that we are using the "worst case" temperature gradient.

Another report of the observation of gravitational species barodiffusion in the aniline and cyclohexane system comes from Giglio and Vendramini [5]. Because they used a shorter sample (1.1 mm tall \times 15 mm wide) the criteria developed above suggest that diffusion should

have dominated convection so long as the horizontal temperature gradient was less than 0.05 K/cm. Giglio and Vendramini did not report their estimate of the temperature gradient in their paper, except to say that the sample cell was a large aluminum block intended to minimize thermal gradients. Since their experiment will tolerate a larger gradient than Maisano, Migliardo, and Wanderligh's, it is likely that our criteria would predict diffusion domination, as was observed.

VIII. SPECULATIONS ON TIME-FLUCTUATING TEMPERATURE GRADIENTS

Going beyond the case with only dc temperature gradients, we consider a conceivable mechanism to move toward equilibrium even from inside the convection regime. This is brought about by the fluctuating convection that would be produced by intermediate-frequency regime temperature gradients. These gradients would effectively randomly rearrange the liquid from time to time. If it happened that one of these fluctuations enhanced the stabilizing vertical density gradient, then all future convection would be damped and thus less able to stir the fluid. Thus if the system takes a step "forward" (toward thermal equilibrium), any later step "backward" would be smaller; it is possible that the system might stumble across the border into the diffusion regime. In order to test this idea it would be convenient to find a system with the crossover to diffusion domination at larger, more readily measured, temperature and density gradients.

We note that Maisano, Migliardo, and Wanderligh mention that the gradients due to barodiffusion formed faster than diffusion would produce them. Giglio and Vendramini's sample evolved with the expected diffusion time scale. We can add our speculations about intermediate-frequency-regime temperature fluctuations to the possible explanations for this extra speed mentioned in Maisano, Migliardo, and Wanderligh's work.

IX. CONCLUSIONS

We have suggested a rough guideline that predicts whether a binary liquid system is likely to evolve toward equilibrium in spite of the convection due to horizontal temperature gradients to which it is subjected. This calculation indicates that temperature gradients that might intuitively seem negligibly small need not be so. Finally our criterion passes a rough comparison with experiment.

We suggest that experimentalists interested in achieving thermal equilibrium as part of other work can look for barodiffusion as a test. Some useful future theoretical work has been proposed. This would include numerical solutions of the Navier-Stokes equations in finite rectangular geometries with velocities reported for very small horizontal temperature gradients. Ideally these could include time-varying temperature gradients as well as constant ones, fixed or free interfaces at the top of the liquid, and a more complete treatment of diffusion, including barodiffusion in a self-consistent manner and the Soret effect. This would provide more accurate velocity-field data than is currently available. This might lead to substantial improvement in the criteria suggested by this

paper. Finally, it would be very interesting to observe barodiffusion in the presence of thermal gradients to test the regime diagram shown in Fig. 2 experimentally.

ACKNOWLEDGMENTS

We wish to acknowledge helpful discussions with N. David Mermin, Eric Siggia, Alain Pumir, Eberhard Bodenschatz, and Dean Ripple as well as support from the National Science Foundation through Low Temperature Physics Grant No. DMR-9001106 and the Material Research Laboratory Central Facilities at Cornell University supported by the NSF under Grant No. DMR-9121654. T.V. acknowledges financial support from the U.S. Department of Education.

APPENDIX: CALCULATION OF THE VELOCITY FIELD

We now present our calculation of the flow in a two-dimensional container of height L and width X containing a two-component liquid subjected to a horizontal temperature gradient. The liquid responds to temperature changes only by thermal expansion, so that the Soret effect is neglected and the Boussinesq approximation has been made. The liquid is assumed to have some constant vertical concentration gradient, with lower densities at the top. Conceptually we consider the infinitely tall slot divided into regions or cells of height L , with temperature difference ΔT between the two sidewalls [13]. The coordinate system, symbols, and scalings are given following Eq. (13). We consider the case where the signs of the temperature difference alternate from a cell to the one above it [13]. We write this temperature as a Fourier series and then for convenience throw out all but the first term [13]. The temperature on the sidewalls is then given by $\pm(2/\pi)\Delta T \cos(\gamma z)$. This is different than the condition that Hart used [$T(x = \pm\frac{1}{2}) = \pm\frac{1}{2}\Delta T$]. Since we have no reason to expect that the horizontal temperature gradients accidentally applied to a container would have any particular character, we do not consider it necessary to require that the temperature be uniform on the sidewalls.

We consider one of these cells as the system under study. Therefore, we require that there be no flow between cells. The temperature at the top and bottom is left free. No molecules are allowed to pass through any wall, so the normal velocity at each side is zero. The tangential velocity goes to zero at the sidewalls (no slip); however, it is more convenient to require that the shear vanish at the top and bottom of the cell (the derivative with respect to the vertical direction of the horizontal velocity is zero) [13].

Taking the incompressible Navier-Stokes equation from Hart

$$\frac{R_a}{P_r} \frac{D\mathbf{u}}{Dt} = -\nabla p + \nabla^2 \mathbf{u} + (T - C)\hat{\mathbf{z}}, \quad (\text{A1})$$

$$R_a \frac{DT}{Dt} = \nabla^2 T, \quad (\text{A2})$$

$$HR_a \frac{\partial C}{\partial t} + \mathbf{R}_s \cdot \hat{\mathbf{u}} = \nabla^2 C, \quad (\text{A3})$$

$$\nabla \cdot \mathbf{u} = 0. \quad (\text{A4})$$

Here $Df/Dt = \partial f/\partial t + \mathbf{u} \cdot \nabla f$, where f is any function, R_a is the Rayleigh number $g\alpha\Delta TX^3/\kappa_T\nu$, P_r is the Prandtl number κ_T/ν , H is the Schmidt number κ_T/D , \mathbf{R}_s is similar to R_s from Eq. (13) except that $(\partial C/\partial z)$ is replaced with ∇C , κ_T is the thermal diffusivity (the diffusion constant for heat), and \mathbf{u} is the velocity vector (w is its vertical component). Because we are interested in the long-time behavior of the system we assume that the flow reaches a steady state so that $\partial f/\partial t = 0$. Also because we are considering the small driving force limit we will consider all the $\mathbf{u} \cdot \nabla f$ terms to be second order and thus negligible, except for $\partial C/\partial z$, which is nonzero as a boundary condition. We neglect $\mathbf{u} \cdot \nabla T$ even though ∇T is also nonzero as a boundary condition because the diffusion of heat is much faster than the diffusion of species, and we are looking for the regime where species convection is of the same speed as species diffusion, and therefore where heat diffusion will still be faster than heat advection.

We then express the velocity as derivatives of a stream function $\Psi(x, z)$, such that $w = u_z = \partial\Psi/\partial x$ (notation Ψ_x) and $u_x = -\Psi_z$. We take the curl of the Eq. (A1), expressing the results in terms of Ψ (remembering that C_z and hence R_s are fixed):

$$\Psi_{xxxx} + 2\Psi_{xxzz} + \Psi_{zzzz} + T_x - C_x = 0. \quad (\text{A5})$$

Equations (A2) and (A3) become

$$T_{xx} + T_{zz} = 0, \quad (\text{A6})$$

$$R_s \Psi_x = C_{xx}. \quad (\text{A7})$$

By integration of Eq. (A7) we get

$$R_s \Psi = C_x, \quad (\text{A8})$$

where we have used the boundary conditions [the conditions are that no diffusion takes place through the sidewalls and that both the normal and tangential velocities are zero at the sidewalls; these are $\Psi(x = \pm\frac{1}{2}, z) = \Psi_x(x = \pm\frac{1}{2}, z) = C_x(x = \pm\frac{1}{2}, z) = 0$] to determine that the constant of integration is zero. Substitution for C_x into Eq. (A5) leaves us with an equation for Ψ with unknowns T and Ψ only. We then assume that $\Psi(x, z)$ has the form $F(x)\cos(\gamma z)$ and $T(x, z) = G(x)\cos(\gamma z)$. The form of Ψ is designed to prevent flow between cells and to observe the free-slip boundary condition at the top and bottom of the cell [13], i.e., $w = 0$ and $\partial u_x/\partial z = 0$ at $z = \pm L/(2X)$. This form for Ψ also anticipates the z dependence of the thermal driving term in Eq. (A5).

The Eq. (A6) yields $G(x) = [2 \sinh(\gamma x)]/[\pi \sinh(\gamma/2)]$, which satisfies the thermal boundary conditions on the sidewalls. This results in the following inhomogeneous differential equation:

$$F_{xxxx} - 2\gamma^2 F_{xx} + (\gamma^4 - R_s)F + \frac{2\gamma}{\pi} \frac{\cosh(\gamma x)}{\sinh(\gamma/2)} = 0. \quad (\text{A9})$$

A particular solution is

$$F_p(x) = E_p \cosh(\gamma x), \quad (\text{A10})$$

where

$$E_p = 2\gamma / [\pi R_s \sinh(\gamma/2)] . \quad (\text{A11})$$

We look for a flow field which circulates about the middle of the cell. Thus we want a vertical velocity that is antisymmetric in x . This means that $F_x(x) = -F_x(-x)$ or $F(x) = F(-x)$. The particular solution has this symmetry.

While the most general solutions to the corresponding homogeneous differential equation are four exponential functions of x with complex wave vectors, this symmetry requirement makes it more convenient to express them as

$$F_h(x) = a_1 \cosh(\mu x) \cos(\lambda x) + a_2 \sinh(\mu x) \sin(\lambda x) . \quad (\text{A12})$$

Here μ and λ are as defined in Eqs. (9) and (10), and we have used the symmetry requirement to eliminate two of the four solutions. Then a_1 and a_2 are chosen so that the total solution (the sum of F_p and F_h) meets the boundary conditions at the sidewalls. This gives

$$a_1 = \frac{2E_p}{\mu \sin(\lambda) + \lambda \sinh(\mu)} \times \{ \gamma \sin(\lambda/2) \sinh(\gamma/2) \sinh(\mu/2) - \cosh(\gamma/2) [\mu \cosh(\mu/2) \sin(\lambda/2) + \lambda \cos(\lambda/2) \sinh(\mu/2)] \} , \quad (\text{A13})$$

$$a_2 = \frac{2E_p}{\mu \sin(\lambda) + \lambda \sinh(\mu)} \times \{ -\gamma \cos(\lambda/2) \cosh(\mu/2) \sinh(\gamma/2) + \cosh(\gamma/2) [\mu \cos(\lambda/2) \sinh(\mu/2) - \lambda \cosh(\mu/2) \sin(\lambda/2)] \} . \quad (\text{A14})$$

Then the appropriate derivatives of $\Psi(x, z)$ are taken to

find the velocity [Eq. (6)] of the flow. If we let the height of the sample go to infinity [and adjust for our use of a temperature difference of $(4/\pi)\Delta T$ instead of ΔT] we recover the velocity expressed by Thangam, Zebib, and Chen and negative one times the velocity printed in Hart. Since it is clear that a liquid that becomes less dense at higher temperatures should rise near the hot wall (Hart's figures agree on this point), we believe that there is a printing error in Hart's article.

We will now briefly describe the nature of the flow we have calculated, emphasizing its dependence on sample height. Tall flows with relatively small vertical density gradients (10^{-8} g/cm⁴, for example) behave like Hart or Thangam-Zebib-Chen flows at the midplane of the cell. The vertical velocity decreases smoothly as one approaches the top and bottom of the container. As we move to shorter samples, the velocity slowly decreases until the sample cell is as tall as it is wide at which point the velocity has gone down by a factor of about 2. Thereafter the velocity falls rapidly. It is down by a factor of 25 when the height is one-tenth the width. As the sample is made shorter, the vertical density gradients are less effective at damping the flow, and again this becomes much more pronounced for samples whose height is less than their width. For systems with very large vertical gradients (10^{-4} g/cm⁴, for example), the velocity actually increases with decreasing height of the container. The velocity rises by a factor of 2 as the sample goes from tall to being of unit height and rises by a further factor of 4 as the height becomes one-tenth the width. In addition to changes in the magnitude the character of the flow also changes. In order for mass to be conserved, an upward or downward flow must have a return flow. For containers with widths less than their heights, the flow at the cold wall serves as the return for the flow at the hot wall while for wide containers the flows at the walls are each recirculated by a separate return flow next to the wall flow on the interior side.

- [1] A. Kumar, H. R. Krishnamurthy, and E. S. R. Gopal, *Phys. Rep.* **98**, 59 (1983).
- [2] R. F. Kayser, M. R. Moldover, and J. W. Schmidt, *J. Chem. Soc. Faraday Trans. 2* **82**, 1701 (1986).
- [3] L. D. Landau and E. M. Lifshitz, *Fluid Mechanics*, 2nd ed. (Pergamon, Oxford, 1987), p. 232.
- [4] M. Giglio and A. Vendramini, *Phys. Rev. Lett.* **34**, 561 (1975).
- [5] M. Giglio and A. Vendramini, *Phys. Rev. Lett.* **35**, 168 (1975).
- [6] G. Maisano, P. Migliardo, and F. Wanderligh, *J. Phys. A* **9**, 2149 (1976).
- [7] D. J. Tritton, *Physical Fluid Dynamics*, 2nd ed. (Clarendon, Oxford, 1988), Chap. 14.
- [8] E. Knobloch and D. R. More, *Phys. Rev. A* **37**, 860 (1988).
- [9] D. A. Nield, *J. Fluid Mech.* **23**, 1918 (1967).
- [10] G. Z. Gershuni and E. M. Zhukhovitskii, *Convective Stability of Incompressible Fluids* (Israel Program for Scientific Translation, Jerusalem, 1976), p. 6.
- [11] J. E. Hart, *J. Fluid Mech.* **49**, 279 (1971).
- [12] S. Thangam, A. Zebib, and C. F. Chen, *J. Fluid Mech.* **112**, 151 (1981).
- [13] Suggested by Alain Pumir (private communication).
- [14] J. Lee, M. T. Hyun, and J. H. Moh, *Numer. Heat Transfer A* **18**, 343 (1990).
- [15] M. E. Thompson and J. Szekely, *Int. J. Heat Mass Transfer* **32**, 1021 (1989).
- [16] P. Berge and P. Calmettes, *Phys. Lett.* **30A**, 7 (1969).
- [17] G. Arcovito, C. Faloci, M. Roberti, and L. Mistura, *Phys. Rev. Lett.* **22**, 1040 (1969).
- [18] B. C. Miller, E. A. Clerke, and S. C. Greer, *J. Phys. Chem.* **87**, 1063 (1983).
- [19] B. A. Scheibner, C. M. Sorensen, D. T. Jacobs, R. C. Mockler, and W. J. O'Sullivan, *Chem. Phys.* **31**, 209 (1978).
- [20] N. Nagarajan, M. K. Tiwari, S. Jyothi, Chandrasekhar Shetty, Anil Kumar, and E. S. R. Gopal, *J. Chem. Thermodyn.* **12**, 907 (1980).
- [21] J. A. Riddick and W. B. Bunger, *Organic Solvents: Physical Properties and Methods of Purification*, 3rd ed., Techniques of Chemistry Vol. 2 (Wiley-Interscience, New York, 1970), pp. 77 and 423.
- [22] G. D'Arrigo, L. Mistura, and P. Tartaglia, *Phys. Rev. A* **1**, 286 (1970).